

Determination of physical parameters in dark mottles

G. Tsiropoula¹ and B. Schmieder²

¹ National Observatory of Athens, Institute of Space Research, Lofos Koufos, GR-15236 Palea Penteli, Greece

² Observatoire de Paris, Section d'Astrophysique de Meudon, F-92195 Meudon Principal Cedex, France

Received 18 December 1996 / Accepted 26 February 1997

Abstract. The application of the cloud model to measurements of the contrast as a function of wavelength in the $H\alpha$ line has recently enabled us to derive numerical values for various parameters (such as velocity, source function, Doppler width and optical depth) of dark mottles observed near the center of the solar disk. The values of these parameters are used together with the calculations of Poland et al. (1971) and Yakovkin and Zel'dina (1975) in order to determine the physical conditions in these structures. Thus population densities at levels 1, 2, 3 (N_1 , N_2 , N_3), total particle density of hydrogen N_H , electron density N_e , electron temperature T_e , gas pressure, total column mass, mass density and degree of hydrogen ionization can be determined. The values obtained are comparable with estimates obtained for spicules and mottles by different authors in the past and, furthermore, offer the prospect of putting observational constraints on non-LTE two-dimensional modelling of dark mottles observed in the $H\alpha$ line which is currently in progress.

Key words: Sun:chromosphere – fine structure – mottles – spicules

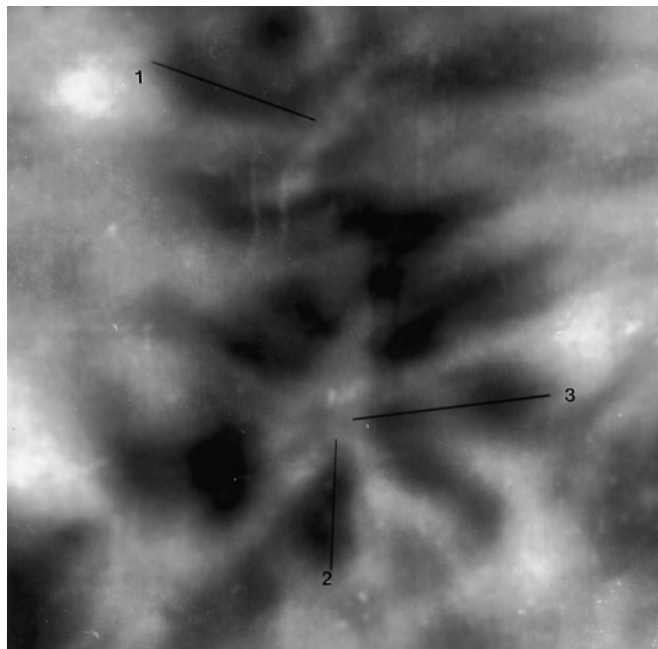


Fig. 1. The rosette region ($33'' \times 33''$) at $H\alpha \pm 0.512 \text{ \AA}$ observed at Pic du Midi with the MSDP on June 17, 1986. The lines mark the axes of 3 dark mottles selected for our analysis.

1. Introduction

Filtergrams of the solar disk in $H\alpha$ show that the chromosphere is rich in features of different intensities, shapes and sizes the variety of which strongly depends on the strength and inclination of the magnetic field. Among these features dark mottles have long been recognized to be one of the basic elements constituting the inhomogeneous character of the chromosphere. They are nearly vertical flux tubes, appear especially enhanced in contrast at $H\alpha \pm 0.5 \text{ \AA}$, and, on the basis of substantial indirect evidence, are believed to be the disk manifestation of spicules.

Knowledge of the physical conditions in isolated chromospheric features, such as filaments, loops, mottles etc., is needed to elucidate the physical processes which are occurring in them. Their determination is, usually, based on the study of the spatial

variation of the emerging radiation intensity, $I(\lambda)$, e.g. on the line profiles. However, the determination of the values of some physical quantities such as velocity, density, pressure etc. from line profiles requires appropriate techniques. A rather convenient and very often used method of extracting information for a large number of absorbing features observed in chromospheric filtergrams is by interpreting their contrast profiles, in terms of the classical Beckers' cloud model (Beckers 1964, Alissandrakis et al. 1990 and references therein). The cloud model offers the attractive possibility of deriving several physical parameters of chromospheric absorbing features, if it can be assumed that these features are sufficiently separated from the chromospheric background. The cloud model is valid only under a restricted set of circumstances and there is no guarantee that these are necessarily obtained in all cases.

Send offprint requests to: G. Tsiropoula

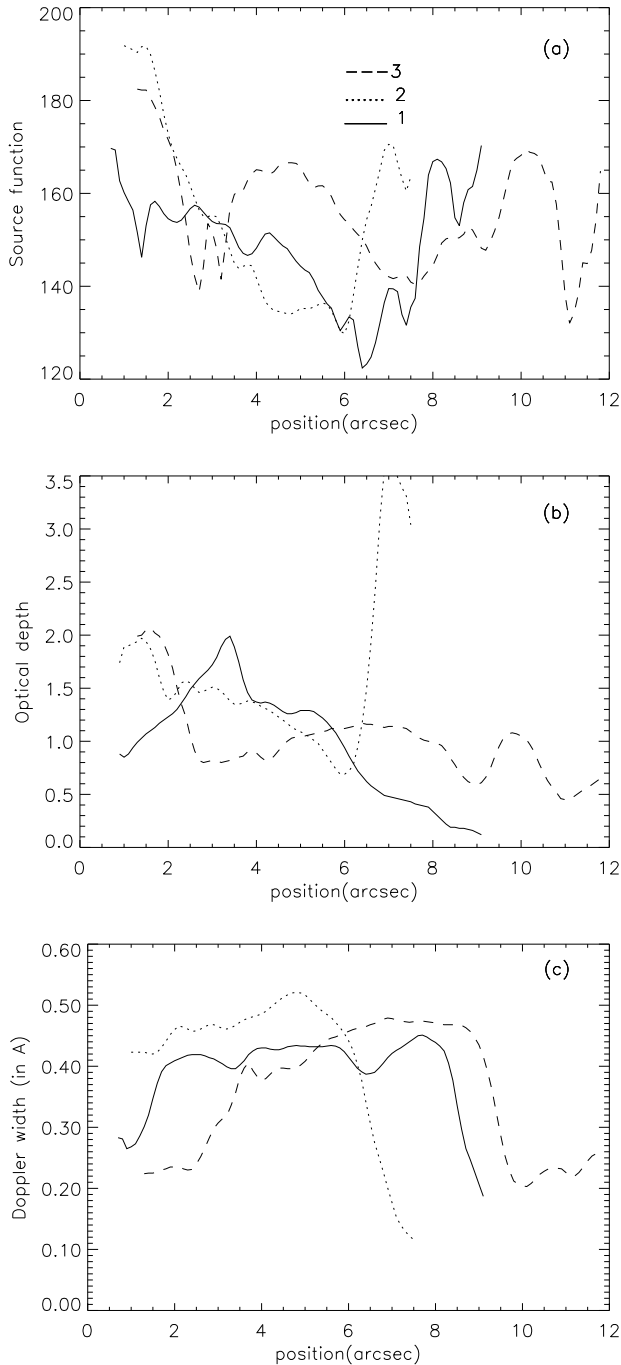


Fig. 2a–c. Variations of the **a** source function, **b** optical depth at line center and **c** Doppler width along the axes of the 3 dark mottles shown in Fig. 1

A significant step forward spectral diagnostics of isolated structures is to take into account the problem of multidimensional radiative transfer in non-LTE. However, it is difficult to apply the non-LTE theory to realistic situations with the necessary rigour, although in recent years various numerical approaches to solve the non-LTE equations have been developed to a high degree of sophistication (Gouttebroze et al. 1993, Auer & Paletou 1994, Heinzel 1995, Paletou 1995, Mein et al. 1996,

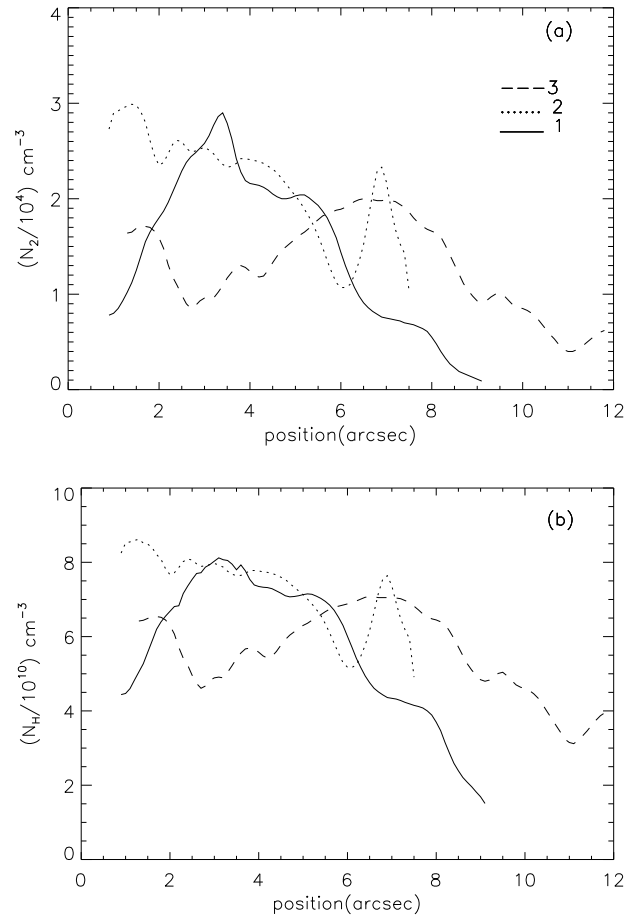


Fig. 3a and b. Variations of **a** N_2 and **b** N_H along the axes of the 3 dark mottles shown in Fig. 1

Paletou 1996). According to these approaches given the input parameters T , p , M and ξ_t (T :kinetic temperature, p :gas pressure, M :total column mass, ξ_t :microturbulent velocity) the problem of constructing non-LTE models reduces to a solution of the radiative transfer equation for each explicitly treated transition, the set of stationary statistical equilibrium equations and constraint equations like total particle-number and charge conservation. As the convergence is faster if one starts with initial values estimated by appropriate techniques, there is a highly desirable need to try to estimate them.

A 2D field of view of a rosette region containing dark mottles, is obtained by the MSDP spectrograph (Mein 1977, Tsiropoula et al. 1993). The observed contrast profiles were matched with theoretical ones using Beckers' cloud model and 4 parameters were derived for the dark mottles (Tsiropoula et al. 1993). The aim of this work is by using the parameters already derived to deduce several physical parameters of these structures in order to give some first estimates of their physical conditions, to put observational constraints to theoretical models and/or, at least, to be used as initial values to non-LTE 2D calculations which are currently in progress (Heinzel, Paletou, 1996, private communication).

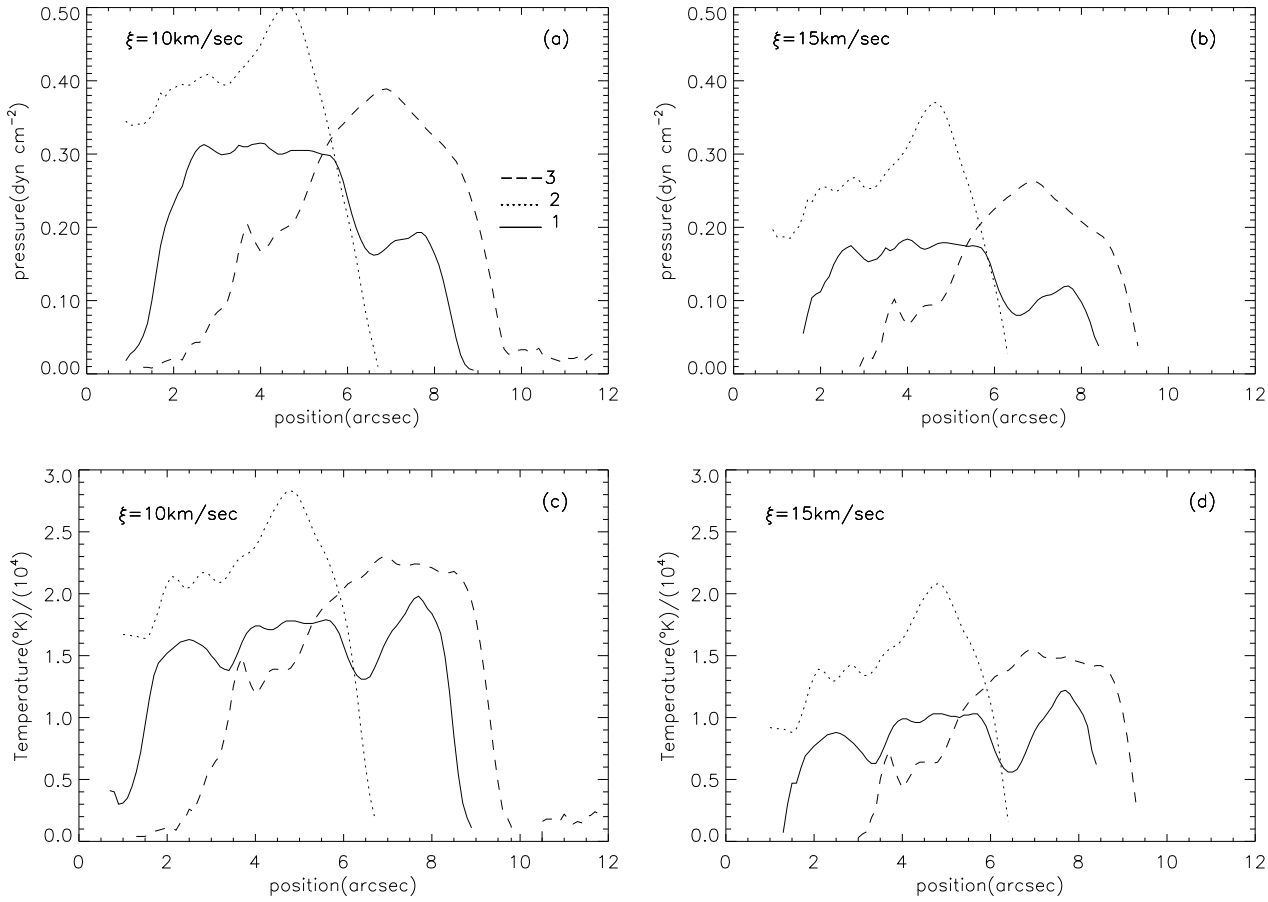


Fig. 4a–d. Variations of p and T for $\xi_t = 10 \text{ km s}^{-1}$ (a, c) and $\xi_t = 15 \text{ km s}^{-1}$ (b, d) along the axes of the 3 dark mottles shown in Fig. 1

2. Derivation of physical parameters in dark mottles

The determination of the physical quantities from the disturbed line intensity (or contrast) profiles is an essential step in understanding the mechanisms of bulk plasma quantities and energy transfer and in the modelling of the inhomogeneous outer atmosphere of the Sun. However, the problem of derivation of fully consistent models from disk observations encounters a number of intrinsic difficulties, because it needs, in general, multi-dimensional solutions of the time-dependent non-LTE transfer equations.

In order to benefit from the large amount of information contained in $\text{H}\alpha$ observations, which still constitute a significant fraction of solar observations, different methods have been proposed to account for the physical processes responsible for the observed pattern of bright and dark features and to derive some physical parameters useful for the modelling of these features. Of the techniques which have been used to study such features the so called cloud model is the one most widely applied. This model considers the feature as a “cloud” overlying a uniform atmosphere. It is suggested that the structure is fully separated from the underlying chromosphere so that the reference “background” profile is meaningful. Furthermore this

background is assumed to be the same below the structure and in the surrounding atmosphere.

The cloud model considers optically thin structures and adopts four adjustable parameters of the contrast profile:

$$\begin{aligned} C(\Delta\lambda) &= \frac{I(\Delta\lambda) - I_o(\Delta\lambda)}{I_o(\Delta\lambda)} \\ &= \left(\frac{S}{I_o(\Delta\lambda)} - 1 \right) (1 - e^{-\tau(\Delta\lambda)}) \end{aligned} \quad (1)$$

where $I_o(\Delta\lambda)$ is the reference profile emitted by the background. In addition, one assumes that the wavelength dependence of the optical thickness is gaussian:

$$\tau(\Delta\lambda) = \tau_o e^{-\left(\frac{\Delta\lambda - \Delta\lambda_I}{\Delta\lambda_D}\right)^2} \quad (2)$$

These parameters, which furthermore are assumed to be constant through the structure, are: the $\text{H}\alpha$ line source function S , the Doppler width $\Delta\lambda_D$, the optical depth at line center τ_o , and the Doppler shift $\Delta\lambda_I$ and can be computed by an iterative least square procedure for non linear functions (Alissandrakis et al. 1990).

Once these parameters are determined the estimation of several other parameters can be made. The absorption coefficient

may be written in the form $\kappa_\lambda = \alpha\phi(\lambda)$, where α , the atomic absorption coefficient, depends only on atomic constants and the number density N_2 of hydrogen atoms in the second quantum level. The absorption profile, $\phi(\lambda)$, if one assumes pure Doppler broadening, is a function of the Doppler width, $\Delta\lambda_D$, and the bulk velocity vector, v . The source function S in complete redistribution, is independent of frequency and depends on the population ratio N_3/N_2 , where N_3 is the number density of hydrogen atoms in the third quantum level. Thus, it is evident that the morphology of H α fine structures arises primarily from the 3-dimensional variation of N_2 , N_3 , v and $\Delta\lambda_D$.

The optical depth at line center may be written:

$$\tau_o = \kappa_o d \quad (3)$$

where κ_o is the line absorption coefficient and d is the path length along the line of sight through the structure. This formula can be written:

$$\tau_o = \frac{\pi^{1/2} e^2 f \lambda^2}{m_e c} \frac{N_2}{c \Delta\lambda_D} d \quad (4)$$

where $f = 0.641$ is the oscillator strength for H α , and m_e is the electron mass. Inserting numerical values in (4) we obtain the following expression for N_2 in terms of the estimated by the cloud model quantities τ_o and $\Delta\lambda_D$:

$$N_2 = 7.26 \cdot 10^7 \frac{\tau_o \Delta\lambda_D}{d} \text{ cm}^{-3} \quad (5)$$

where $\Delta\lambda_D$ is in Å and d is in km.

Yakovkin and Zel'dina (1975) considering vertical slabs solved the statistical equilibrium equations for the $n = 2$ level assuming its population and depopulation through the Balmer continuum as the dominant population mechanism and suggested that given N_2 , the electron density, N_e , can be determined from the relation:

$$N_e = 3.2 \cdot 10^8 \sqrt{N_2} \text{ cm}^{-3} \quad (6)$$

To the same relation one can arrive from the results of Giovanelli (1967a). Thus once N_2 is estimated from the relation (5) we can have an estimation of the electron density from the relation (6), provided that we know the thickness of the structure. We must say that although the populations vary with position through the slab due to the change in the Lyman continuum source function Eq. (5) and (6) can only give the volume averages of these populations over the thickness of the slab.

Poland et al. (1971) using vertical slab model atmospheres irradiated from both sides and a model atom of two bound levels and a continuum have determined the ionization and excitation equilibrium for hydrogen. They arrived at the same relation between N_e and N_2 as the one given by Yakovkin and Zel'dina. They also showed that for most models there is a single-valued relation between N_H , the total particle density of hydrogen (i.e., neutral plus ionized), and N_2 (see also their Fig. 5). We find this relation (for the linear part of the curves) to be:

$$N_H = 5 \cdot 10^8 \cdot 10^{0.5 \log N_2} \quad (7)$$

We must comment here that Giovanelli (1967a,b), Poland et al. 1971 and Yakovkin and Zel'dina (1975) considered vertically-standing 1D slabs of finite geometrical thickness D illuminated by the surrounding atmosphere. It might seem that for structures observed against the solar disk instead of vertical geometry a horizontal slab irradiated from below should be considered. Although this kind of radiative modelling is now in progress, no relations between the quantities we want are published. We shall return to the question of the geometry later on the discussion.

Once the densities N_e and N_H are determined, from the constraint of particle conservation and assuming a mixture of the hydrogen and helium atoms in the structure, we can write for the hydrogen ground-level population, N_1 :

$$N_1 = \frac{[N_t - (2 + \alpha)N_e]}{1 + \alpha} \quad (8)$$

where N_t is the total particle number density and α is the abundance ratio of helium to hydrogen (≈ 0.0851).

From N_2 and the source function obtained from the cloud model one can determine N_3 from the relation:

$$S = \frac{2h\nu^3}{c^2} \frac{1}{\frac{N_2 g_3}{N_3 g_2} - 1} \quad (9)$$

From the calculated Doppler width values and if we assume a value for the microturbulent velocity ξ_t we can deduce the temperature, T_e .

Once the above values are determined derivation of several other parameters is straightforward. Thus the gas pressure is:

$$p = k(N_e + 1.0851N_H)T_e \quad (10)$$

and the total column mass

$$M = (N_H m_H + 0.0851N_H \times 3.97m_H) d \quad (11)$$

where m_H is the mass of the hydrogen atom. The mass density is then:

$$\rho = \frac{M}{d} \quad (12)$$

and the degree of hydrogen ionization:

$$x_H = \frac{N_e}{N_H} \quad (13)$$

3. Observations and results

The observations of a rosette region consisting of several dark mottles located almost at the disk center (N5, W5) were made with the Multichannel Double Pass (MSDP) Spectrograph mounted on the 50 cm "Tourelle" refractor of the Pic du Midi Observatory, on June 17, 1986 (for details on these observations see Schmieder et al. 1991, Tsiropoula et al. 1993). The MSDP having 11 channels provides at every point of the field of view the profile of the H α line which can be reconstructed from 11

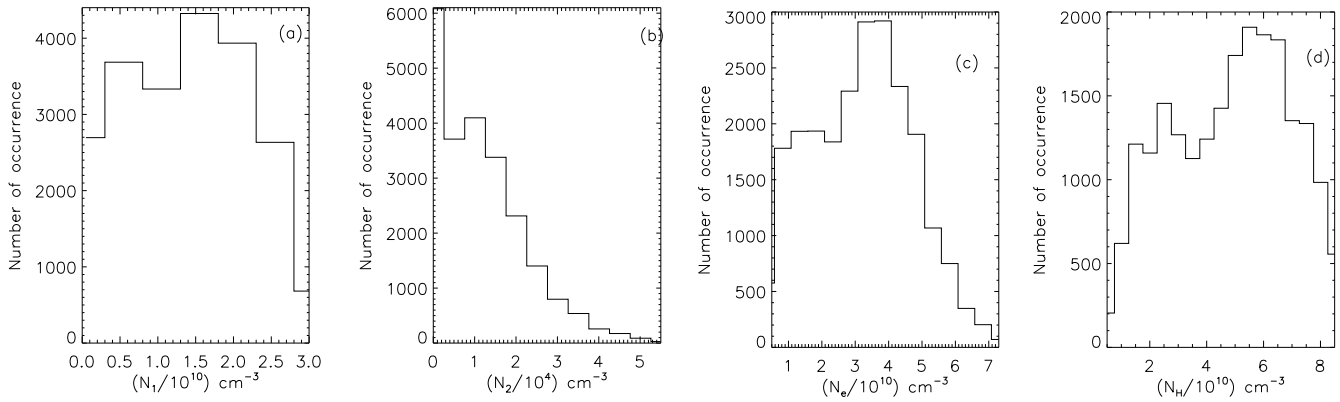


Fig. 5a–d. Histograms of **a** N_1 , **b** N_2 , **c** N_e , **d** N_H for the whole region of Fig. 1

values. Thus the processed MSDP spectra can be used for the computation of two dimensional intensity and Doppler velocity maps at several depths in the line.

The duration of the present observations was 15 min. From the entire sequence one frame of very good quality was selected for the present study (Fig. 1) and the cloud model was applied. After the derivation of the 4 cloud model parameters one can construct 2D maps of these (Tsiropoula et al., 1993) and of all the other quantities based on these.

In order to show the variations of the physical parameters along the axes of distinct dark mottles their values were averaged along a strip extending $0.3''$ on either side of a central axis. The step along the axis was $0.1''$. The variation of the 3 parameters determined by the cloud model e.g. source function, optical depth and Doppler width, along the axes of 3 dark mottles marked in Fig. 1 is shown in Fig. 2. The source function follows the behavior of the contrast: it is larger at both edges of the structures and smaller along their central body. Considering the source function variations we take the outer edge (e.g. away from the center of the rosette) to be at $\approx 8''$ for mottle 1 at $\approx 6.8''$ for mottle 2 and at $\approx 10''$ for mottle 3. After this distance the local background is reached. The optical depth shows no clear behavior, while the Doppler width is almost constant along a great part of the axes of mottles; it diminishes towards the two edges of all mottles.

The derivation of the other physical parameters is done through the relations (5) to (13) given above. Taking the thicknesses of the structures to be equal to 1000 km, a value typical for dark mottles, and the angle between their central axes and the line of sight equal to the mean inclination given for spicules by Heristchi and Mouradian (1992), e.g. equal to 30° , we have a path length along the line of sight equal to 2000 km. The source function is given by the cloud model in $1/1000$ of the nearby disk-center continuum intensity. In order to calculate N_3 from the relation (9) this intensity was taken equal to $4.077 \cdot 10^{-5}$ cgs (Pierce & Allen 1977). The populations vary markedly with position along the structures 1 and 2 but remain almost constant along structure 3 (Fig. 3a,b). The Doppler width is rather high, which implies rather high temperature and/or large microturbulent velocity. For the derivation of the temperature from the

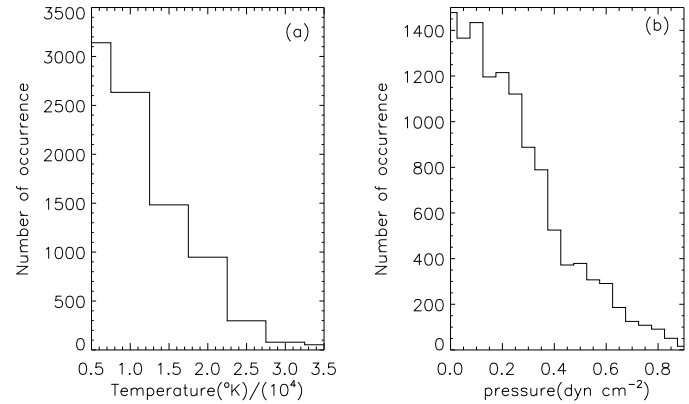


Fig. 6a and b. Histograms of **a** T and **b** p for the whole region of Fig. 1 assuming $\xi_t = 15 \text{ km s}^{-1}$.

Doppler width we have assumed two different values for the microturbulent velocity, ξ_t (e.g. 10 km s^{-1} and 15 km s^{-1}) in order to show its effect on the values of the temperature and pressure. The variations of the pressure and temperature along the same structures are shown in Fig. 4. Smaller values of ξ_t lead to greater values of pressure and temperature at ≈ 1.7 times. In any case the values of pressure are smaller than 0.5 dyn cm^{-2} .

It is obvious from the variation of pressure, that we are far from hydrostatic equilibrium and that the magnetic field plays an important role in dark mottles in supporting the material against gravity. The mean values and standard deviations of the different estimated parameters are given in Table 1, while histograms of N_1 , N_2 , N_e , N_H , T and p for the whole region of Fig. 1 are given in Fig. 5 and 6.

4. Diagnostic results for mottles and spicules

It is of interest to compare some of the above derived values with estimates obtained for spicules and mottles by different authors in the past.

Table 1. Physical parameters of dark mottles

Parameter	Average value	Standard deviation
N_1, cm^{-3}	$1.6 \cdot 10^{10}$	$8.3 \cdot 10^9$
N_2, cm^{-3}	$1.4 \cdot 10^4$	$1.1 \cdot 10^4$
N_3, cm^{-3}	$1.6 \cdot 10^2$	$1.3 \cdot 10^2$
N_H, cm^{-3}	$5.1 \cdot 10^{10}$	$2.1 \cdot 10^{10}$
N_e, cm^{-3}	$3.4 \cdot 10^{10}$	$1.5 \cdot 10^{10}$
T, K (for $\xi_t = 10 \text{ km s}^{-1}$)	$1.4 \cdot 10^4$	$9.2 \cdot 10^3$
T, K (for $\xi_t = 15 \text{ km s}^{-1}$)	$1.0 \cdot 10^4$	$7.7 \cdot 10^3$
$p, \text{dyn cm}^{-2}$ (for $\xi_t = 10 \text{ km s}^{-1}$)	0.20	0.1
$p, \text{dyn cm}^{-2}$ (for $\xi_t = 15 \text{ km s}^{-1}$)	0.15	0.1
$M, \text{g cm}^{-2}$	$2.2 \cdot 10^{-5}$	$9.4 \cdot 10^{-6}$
$\rho, \text{g cm}^{-3}$	$1.1 \cdot 10^{-13}$	$4.7 \cdot 10^{-14}$
x_H	0.65	0.1

4.1. a. Spicules

Giovanelli (1967a,b) was the first who made qualitative non-LTE computations of the H α and Ca II K lines for spicules and mottles. He arrives at a spicule model in which $T = 20000 \text{ K}$ and $N_e = 3 \cdot 10^{10} \text{ cm}^{-3}$ at a height of 6000 km (1967b). Using the same computations for Ca II but somewhat modified data, Beckers (1972) arrives at a model in which T increases from 9000 K at 2000 km to 16000 K at 8000 km. N_e decreases over this height interval from $1.6 \cdot 10^{11}$ to $4.3 \cdot 10^{10} \text{ cm}^{-3}$. Avery and House (1969) used a Monte-Carlo technique to compute the K-line profile emergent from a spicule. The resultant model is characterized by an outward increase in T from 6000 K near the base to 15000 K near the top. Electron density decreases outwards from $8 \cdot 10^{11} \text{ cm}^{-3}$ at the base to $4 \cdot 10^{10} \text{ cm}^{-3}$ at the top. In order to produce the observed widths of the profiles a microturbulent velocity of 20 km s^{-1} is needed. Alissandrakis (1973) analyzing simultaneous spectra of spicules in H α , H β and CaII K derived an average electron density of $9 \cdot 10^{10} \text{ cm}^{-3}$ and an average electron temperature of 13000 K at a height of 5400 km above the limb. He also suggested a value for the microturbulent velocity equal to 20 km s^{-1} . Values of N_3 for H given by Zirker (1962) decrease from 69 cm^{-3} at 6000 km to 10 at 8600 km, which are too low. From the excitation tables given by Giovanelli (1967a) we find that for $T = 10^4 \text{ K}$ and N_e in the range $10^{10} - 10^{11} \text{ cm}^{-3}$ the corresponding values of N_3 are found in the range $5.6 - 622 \text{ cm}^{-3}$. From the excitation tables of Giovanelli (1967a) one can see that the values of N_3 given by Zirker lead to considerably lower values of N_e . Evidently, the N_3 values given by Zirker are too low.

4.2. Mottles

Excitation and ionization of H in slab geometries illuminated by coronal and chromospheric radiation have been studied among others by Giovanelli (1967a,b) and Poland et al. (1971). These authors found that the populations of the N_2 and N_3 levels of hydrogen are nearly independent of the temperature in the range

6000 to 20000 K and are closely proportional to N_e^2 for $10^{10} \leq N_e \leq 10^{12}$.

The drawback of Giovanelli's analysis is that (i) he uses only the line center contrast and (ii) he neglects any velocity fields. As his computations are pioneering as far as the fine-scale chromospheric modelling and non-LTE calculations are concerned he could not make more but a rough estimate of the range of T and N_e . He has concluded that:

- $T < 10000 \text{ K}$, $N_e \approx 2 \cdot 10^{11} \text{ cm}^{-3}$ for dark mottles
- $T < 20000 \text{ K}$, $N_e \approx 10^{11} \text{ cm}^{-3}$ for less opaque mottles and
- $T > 25000 \text{ K}$, $N_e \approx 5 \cdot 10^{10} - 10^{11} \text{ cm}^{-3}$ for bright mottles.

Tsiropoula et al. (1993) based on some parameters given by the cloud model estimated the electron densities within dark mottles in the range $4 - 5 \cdot 10^{10} \text{ cm}^{-3}$ and the temperature in the range 7100 - 13000 K.

Quite recently Heinzel & Schmieder (1994) using the non-LTE calculations of Gouttebroze et al. (1993) for vertically-standing 1D prominence-like slabs irradiated from both sides by an isotropic incident radiation, found that two solutions exist for a given negative contrast: one at lower pressures ($< 0.5 \text{ dyn cm}^{-2}$) and the other at higher pressures. They favoured the higher pressure solution and concluded that H α profiles of dark mottles can easily be interpreted with temperatures less than 10^4 and electron densities of the order of 10^{11} .

Based on these different estimates, and if we do not consider Giovanelli's results about T_e and N_e the accuracy of which is rather low, it seems that (a) the physical conditions inside the dark mottles are very similar to those in spicules, (b) temperatures in dark mottles and spicules are in the range 7000 - 15000 K and electron densities in the range $4 \cdot 10^{10} - 10^{11}$.

5. Discussion and conclusions

A method has been described which under appropriate circumstances enables the determination of several physical parameters of the dark mottles. This method can also be applied to other elevated dark structures observed in H α like fibrils or arch filaments.

The values obtained by this method are comparable with the values given by different authors for spicules and mottles (Sect. 4). It seems that dark mottles have mean temperature less than 14000 K and mean pressure less than 0.5 dyn cm^{-2} (note that these values depend strongly on the adopted value of the microturbulent velocity). These values together with the values of the other physical parameters of Table 1 can be used as first estimates of the physical conditions existing in mottles and also as initial values in non-LTE models.

It should be noted that the reliability of the determination of the various physical parameters depends on a number of factors. One important question is the problem of the geometry. Giovanelli (1967a,b), Poland et al. 1971, Yakovkin and Zel'dina (1975) considered 1D-slab models of finite horizontal thickness. Actually, mottles are plasma structures confined by the magnetic field and extending to the corona. Their geometry resembles long cylinders inclined at various angles to the solar surface. As demonstrated by Gouttebroze (1989) differences

between the source function computed for 1D-cylinders of diameter D and an equivalent 1D-slab are not critically important. For 1D-cylinders, no multilevel non-LTE models with partial redistribution exist so far. 2D prominence-like slabs as seen at the limb have recently been studied in some detail (Paletou 1995), but this again is not the case for the structures under study. Thus the use of the results of the works mentioned above where the mottles are approximated by 1D vertical slabs is primarily dictated by their availability. But, it is obvious that more progress is needed towards multidimensional radiative transfer modelling.

Another question which may arise is the validity of applying the cloud model to derive values for S , $\Delta\lambda_D$, and τ_o . Cram (1986) has examined the self consistency between the values of S inferred by the application of the cloud model and those calculated using the non-LTE theory of formation of $H\alpha$ and found a satisfactory agreement for most of them. Heinzel and Schmieder (1994) using non-LTE models have concluded that for low pressure structures ($< 0.5 \text{ dyn cm}^{-2}$) one can easily apply the classical cloud model assuming a constant source function and rather low opacity, while the higher pressure solution gives much higher opacity and strongly non-constant source function. However, it should be noted that they used for their computations as initial value a microturbulent velocity equal to 5 km s^{-1} . This value is probably suitable for prominence models, but, according to different authors, it seems to be too low for spicules and mottles, for which values as large as 25 km s^{-1} are reported. The value of the microturbulent velocity is crucial in the determination of the Doppler width and thus in the estimation of the temperature and pressure. Another point of uncertainty arises from the determination of the path length, d . The error in the determination of N_2 and M is proportional to the error in d , while the percentage error in N_e is one half the percentage error in N_2 .

Although we now have a good qualitative description of the morphology and evolution of chromospheric fine structures less progress has been made in the development of techniques for diagnosing their physical conditions. As these structures can be regarded as basic constituents of the solar atmosphere the detailed understanding of their physical behavior plays a

crucial role in the modelling of an inhomogeneous atmosphere as a whole. As new large instruments (SOHO, THEMIS) provide us with a great wealth of high quality spectroscopic data, new efficient tools for spectral diagnostics are highly desirable.

Acknowledgements. The authors are indebted to Dr P. Heinzel and P. Mein for useful comments and discussion and to R. Hellier and C. Coutard for the observations. Travel funds for this work were provided in part through the bilateral exchange program between France and Greece.

References

- Alissandrakis C. E., 1973, *Solar Phys.* 32, 345
 Alissandrakis C. E., Tsiropoula G., Mein P., 1990, *A&A* 230, 200
 Auer L.H., Paletou F., 1994, *A&A* 285, 675
 Avery L.W., House L.L., 1969, *Solar Phys.* 10, 88
 Beckers J. M., 1964, Ph. D. Thesis, Utrecht
 Beckers J. M., 1972, *ARAA* 10, 73
 Cram L.E., 1986, *ApJ* 301, 989
 Giovanelli R.G., 1967a, *Aust. J. Phys.* 20, 81
 Giovanelli R.G., 1967b, in: Xanthakis J.N. (ed.) *Solar Physics, Inter-science*, London
 Gouttebroze P., Heinzel P., Vial J.-C., 1993, *A&A* 99, 513
 Heinzel P., Schmieder B., 1994, *A&A* 282, 939
 Heinzel P., 1995, *A&A* 299, 563
 Heristchi D., Mouradian Z., 1992, *Solar Phys.* 142, 21
 Mein P., 1977, *Solar Phys.* 54, 55
 Mein N., Mein P., Heinzel P., Vial J.-C., Malherbe J.M. and Staiger J., 1996, *A&A* 309, 275
 Paletou F., 1995, *A&A* 302, 587
 Paletou F., 1996, *A&A* 311, 708
 Pierce A.K., Allen R.G., 1977, in: White O.R. (ed.) *Solar Output and its Variations*, Colorado Univ. Press, Boulder, p. 169
 Poland A., Skumanich A., Athay R.G. & Tandberg-Hanssen E., 1971, *Solar Phys.* 18, 391
 Schmieder B., Raadu M. A., Wiik, J. E., 1991, *A&A* 252, 353
 Tsiropoula G., Alissandrakis C. E. and Schmieder B., 1993, *A&A* 271, 574
 Yakovkin N.A., Zel'dina M. Yu., 1975, *Solar Phys.* 45, 319
 Zirker, J. B., 1962, *ApJ* 136, 250